Statistical Thermodynamics of Mixtures of Rodlike Particles. 4. The Poisson Distribution

Randall S. Frost and Paul J. Flory*

Department of Chemistry, Stanford University, Stanford, California 94305.
Received June 8, 1978

ABSTRACT: Biphasic equilibria in systems comprising rodlike solute particles having a Poisson distribution of lengths, these being in admixture with a solvent, are treated by adaptation of theoretical relationships presented in the preceding papers. Selective partitioning of solute species between coexisting isotropic and anisotropic phases occurs, but its effect diminishes as the average length $\bar{x}_n^0$ (or axis ratio) of the rodlike particles increases and the polydispersity of the Poisson distribution simultaneously decreases. The biphasic gap is much narrower than for the most probable distribution. When $\bar{x}_n^0$ is large, concentrations of the coexisting phases and other characteristics of the heterogeneous system formed from a Poisson distribution of solute species conform closely to those for the binary mixture of solvent and monodisperse rods with axis ratio $x = \bar{x}_n^0$.

The partitioning of a Poisson distribution of rodlike solute species between isotropic and anisotropic phases is treated in this paper. The analysis parallels that for the most probable distribution presented in the preceding paper,[1] here designated part 3. Owing to the much narrower breadth of the Poisson distribution, however, the results deduced depart markedly from those in 3 for the most probable distribution.

We define the distribution according to the number $x - 1$ of segments beyond the first in a given molecule, or particle. The segments beyond the initial member of each molecule may be considered to have been stochastically distributed at random over a fixed number n_2 of solute particles.[2] Defined in this way, the lowermost species of the distribution has $x = 1$ (rather than 0) and the number of x-meric species is

$$n_x^0 = n_2^0 e^{-\nu}\nu^{x-1}/(x-1)! = n_2^0 \nu^{-1} e^{-\nu} x \nu^x / x! \quad (1)$$

Since

$$\sum_1^\infty n_x^0 = n_2^0$$

and

$$\sum_1^\infty x n_x^0 = n_2^0(\nu + 1)$$

it follows that

$$\bar{x}_n^0 = \nu + 1 \quad (2)$$

which identifies ν as the average number of segments beyond the first. The ratio of the weight to the number average is given by[2]

$$\bar{x}_w^0/\bar{x}_n^0 = 1 + \nu/(\nu+1)^2 \quad (3)$$

Its small departure from unity attests to the narrowness of the Poisson distribution. As ν, and therefore $\bar{x}_n^0$, increase indefinitely, this ratio converges to unity.

The volume fractions in the parent distribution are given by

$$v_x^0/v_2^0 = x n_x^0/\sum x n_x^0 = [e^{-\nu}/\nu(\nu+1)]x^2\nu^x/x! \quad (4)$$

Theory

1. General Relationships. The conservation eq 3-3, -4, and -5 are directly applicable. Equations 3-5′ and 3-6 are replaced by

$$\Phi v_x + (1-\Phi)v_x' = v_2^0 e^{-\nu}\nu^x x^2/\nu(\nu+1)x! \quad (5)$$

and

$$\Phi v_2/\bar{x}_n + (1-\Phi)v_2'/\bar{x}_n' = v_2^0/(\nu+1) \quad (6)$$

where Φ is the ratio of the volume of the isotropic phase to the total volume.

Substitution of eq 1-35[3] for solute species with $x \leq y = y_{eq}$ into eq 5 yields (compare eq 3-7)

$$v_x'/v_2^0 = e^{-\nu}\nu^x x^2/x!\Phi\nu(\nu+1)[e^{\zeta x} - (1 - 1/\Phi)], \quad x \leq y \quad (7)$$

with ζ defined by eq 1-36. Hence, the combined volume of all species $x \leq y$ in the anisotropic phase is

$$v_{2R}' = v_2^0 I_{1R}/\Phi\nu(\nu+1) \quad (8)$$

and

$$\bar{x}_{nR}' = I_{1R}/I_{0R} \quad (9)$$

with I_{0R} and I_{1R} defined by

$$I_{mR} \equiv e^{-\nu}\sum_1^{x\leq y} x^{1+m}\nu^x/x![e^{\zeta x} - (1 - 1/\Phi)] \quad (10)$$

where $m = 0$ or 1. Equation 8 corresponds to eq 3-8 with $(1-p)^{-2} = \bar{x}_n^2$ replaced by $\nu(\nu+1) = (\bar{x}_n - 1)\bar{x}_n$. Equation 9 is identical with 3-10.

Similarly, for species with $x > y$, one obtains from eq 5 and 1-38

$$v_x'/v_2^0 = (y/e)^2 e^{-\nu}\nu^x x^2/x!\Phi\nu(\nu+1) \times [x^2 e^{-\eta x} - (y/e)^2(1 - 1/\Phi)], \quad x > y \quad (11)$$

η being defined by eq 1-39 or -40. Hence,

$$v_{2A}' = v_2^0 I_{1A}(y/e)^2/\Phi\nu(\nu+1) \quad (12)$$

(compare eq 3-13) and

$$\bar{x}_{nA}' = I_{1A}/I_{0A} \quad (13)$$

where

$$I_{mA} \equiv e^{-\nu}\sum_{x>y} x^{1+m}\nu^x/x![x^2 e^{-\eta x} - (y/e)^2(1 - 1/\Phi)] \quad (14)$$

Equations 3-17 relating v_2' to v_{2R}' and to v_{2A}', and eq 3-18 or -18′ relating $\bar{x}_n'$ to $\bar{x}_{nR}'$ and to $\bar{x}_{nA}'$ may be employed without alteration. Likewise, eq 3-19, relating y to v_{2A}' and to $\bar{x}_{nA}'$, and eq 3-20, -20′, and -21 are applicable to the partitioned Poisson distribution.

The relationships in this section together with those cited from 3 may be solved numerically for given values of ν and Φ according to the procedure outlined in 3; see section 2 of that paper.[1]

The sums I_{0A} and I_{1A}, unlike those for the partitioned most probable distribution, do not diverge when $\Phi \to 1$. Hence, the foregoing equations for the Poisson distribution hold for $0 < \Phi \leq 1$. Only in the limit $\Phi = 0$ are modifications required.

0024-9297/78/2211-1134$01.00/0

2. The Limiting Case $\Phi = 0$. In this limit $v_x' = v_x^0$, $v_2' = v_2^0$, and $\bar{x}_n' = \bar{x}_n^0 = \nu + 1$. Equations 4 and 1-35 give

$$v_x = v_2'[e^{-\nu}/\nu(\nu + 1)]x^2b^x/x!, \quad x \leq y \tag{15}$$

where $b = \nu \exp(\zeta)$, and from eq 4 and 1-38

$$v_x = v_2'[(e/y)^2e^{-\nu}/\nu(\nu + 1)]x^4a^x/x!, \quad x > y \tag{16}$$

where $a = \nu \exp(-\eta)$. Equations 15 and 16 correspond to eq 3-45 and 3-46, respectively. It follows that (compare eq 3-47, -48, -49, and -50)

$$v_2 = v_2'J_1/\nu(\nu + 1) \tag{17}$$

and

$$\bar{x}_n = J_1/J_0 \tag{18}$$

where

$$J_m = e^{-\nu}(e/y)^2\sum_1^\infty x^{3+m}a^x/x! + e^{-\nu}\sum_1^{y^*}[x^{1+m}b^x - (e/y)^2x^{3+m}a^x]/x! \tag{19}$$

with y^* the largest interger $\leq y$. Equations 17 and 18 correspond to 3-49 and 3-50, respectively. Evaluation of the infinite sum in eq 19 for $m = 0$ and 1 leads to

$$J_0 = e^{-\nu}(e/y)^2a(a^2 + 3a + 1)e^a + e^{-\nu}\sum_1^{y^*}[xb^x - (e/y)^2x^3a^x]/x! \tag{20}$$

and

$$J_1 = e^{-\nu}(e/y)^2a(a^3 + 6a^2 + 7a + 1)e^a + e^{-\nu}\sum_1^{y^*}[x^2b^x - (e/y)^2x^4a^x]/x! \tag{21}$$

Substitution of eq 4 into

$$v_{2A}' = v_2' - \sum_1^{y^*} v_x'$$

with $v_x^0 = v_x'$ and $v_2^0 = v_2'$ yields

$$v_{2A}' = v_2'\{1 - [e^{-\nu}/\nu(\nu + 1)]\sum_1^{y^*}x^2\nu^x/x!\} \tag{22}$$

which corresponds to eq 3-51. According to eq 3-18 with $\bar{x}_n' = \bar{x}_n^0 = \nu + 1$

$$1/\bar{x}_{nA}' = (v_2'/v_{2A}')[(\nu + 1)^{-1} - v_{2R}'/v_2'\bar{x}_{nR}']$$

Substitution of eq 8, 9, and 10 with $v_2^0 = v_2'$ followed by substitution of $\Phi = 0$ gives

$$1/\bar{x}_{nA}' = [v_2'/v_{2A}'(\nu + 1)][1 - e^{-\nu}\nu^{-1}\sum_1^{y^*}x\nu^x/x!] \tag{23}$$

which corresponds to eq 3-52. Equation 3-53 holds without alteration.

These equations together with eq 3-19 and 3-20′ may be solved numerically for a given value of ν according to the procedure indicated for solution of the corresponding equations in 3.

3. Undiluted Systems. In undiluted systems numerical calculations show that $y_{eq} < 1$ for any value of $\nu = \bar{x}_n^0 - 1$ sufficiently large for existence of a stable anisotropic phase. Hence, $v_{2R}' = 0$; the sum in eq 14 runs from 1 to ∞ and I_{mA} may be written I_m; and the finite sums in eq 20 and 21 vanish. Equation 12 yields

$$\Phi = (y/e)^2I_1/\nu(\nu + 1) \tag{24}$$

which corresponds to eq 3-59. Equations 3-60 and -61 hold without revision, and adaptation of eq 3-62 is achieved by replacing $1 - p$ by $(\nu + 1)^{-1}$. The resulting set of equations may be solved numerically in the manner indicated in 3.

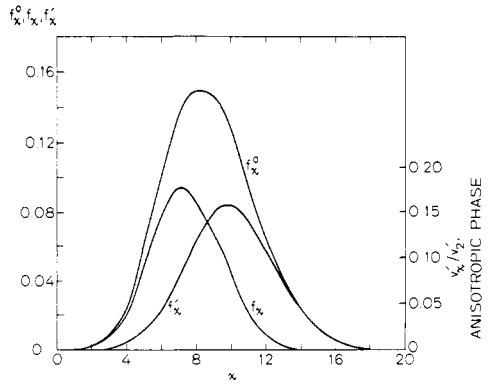

Figure 1. Partitioning of solute species between isotropic (f_x) and anisotropic (f_x') phases for a Poisson distribution (f_x^0) with $\bar{x}_n^0 = \nu + 1 = 8$ shown by the upper curve, the volumes of the coexisting phases being equal ($\Phi = 0.50$). The f_x' curve referred to the ordinate axis on the right-hand side represents the distribution v_x'/v_2' within the anisotropic phase.

The unique solution at incipient separation of an anisotropic phase, i.e., at $\Phi = 1$, is: $\bar{x}_n = 5.1643$, $y = 0.9028$, and $\bar{x}_n' = 8.2737$.

The unique solution at $\Phi = 0$ may be obtained as follows from the equations of the preceding section. Inasmuch as the finite sums in eq 20 and 21 vanish in the present case, substitution of these equations into eq 17 and 18, respectively, yields

$$\nu(\nu + 1)e^\nu(y/e)^2 = a(a^3 + 6a^2 + 7a + 1)e^a \tag{25}$$

and

$$\bar{x}_n = (a^3 + 6a^2 + 7a + 1)/(a^2 + 3a + 1) \tag{26}$$

Substitution of $v_2 = v_2' = v_{2A}' = 1$ and $\bar{x}_n' = \nu + 1$ in eq 1-20′ followed by substitution of eq 26 for $\bar{x}_n$ and replacement of η by $\ln(\nu/a)$ according to the definition of a yields

$$\ln \nu + (y - 1)/(\nu + 1) = a(a^2 + 5a + 4)/(a^3 + 6a^2 + 7a + 1) + \ln a \tag{27}$$

According to eq 3-60

$$\nu = y \exp(2/y) - 1 \tag{28}$$

Elimination of ν from eq 25 and 27 by use of eq 28 yields two equations in y and a. Their solution gives $y = 0.93488$ and $a = 3.04077$. It follows that $\bar{x}_n' = \nu + 1 = 7.9405$ is required at the threshold $\Phi = 0$ in an undiluted system, and, for the incipient isotropic phase, $\bar{x}_n = 5.4665$ according to eq 26.

Results of Numerical Calculations

Distributions of species in the coexisting phases for $\nu = 7$ and $\Phi = 0.5$ calculated according to the relations and procedure in section 2 above are shown in Figure 1. The curves for f_x and f_x', when referred to the ordinate on the left, represent ratios of volumes of x-mer in the respective phases to the total volume of all solute species in both phases (see eq 3-73 and -74). The upper curve, being the sum of the lower two, shows the parent Poisson distribution. When referred to the ordinate on the right, the curve for f_x' describes the distribution v_x'/v_2' in the anisotropic phase. (Compare with Figure 1 of part 3.) The distributions in the coexisting phases for $\nu = 7$ at $\Phi = 0.9$ are shown in Figure 2.

The shapes of the curves for f_x and f_x' in Figures 1 and 2 are similar to one another. They are somewhat narrower than the parent Poisson distribution f_x^0, however. Fractionation of species between the phases is most readily

Table I
Parameters for Coexisting Phases for the Poisson Distribution with $\nu = 7$

Φ	y	v_2	v_2'	$\bar{x}_n$	$\bar{x}_n'$	$\bar{x}_w/\bar{x}_n$	$\bar{x}_w'/\bar{x}_n'$
0	0.9402	0.9931	0.9981	5.512	8.000	1.1128	1.1094
0.2	1.0299	0.9134	0.9734	6.201	8.584	1.0997	1.0901
0.5	1.1253	0.8391	0.9450	6.897	9.324	1.0951	1.0778
0.8	1.2110	0.7745	0.9169	7.518	10.214	1.0981	1.0740
0.9	1.2392	0.7498	0.9062	7.740	10.662	1.1015	1.0758
1.0	1.2478	0.7123	0.8940	8.000	11.702	1.1094	1.0947

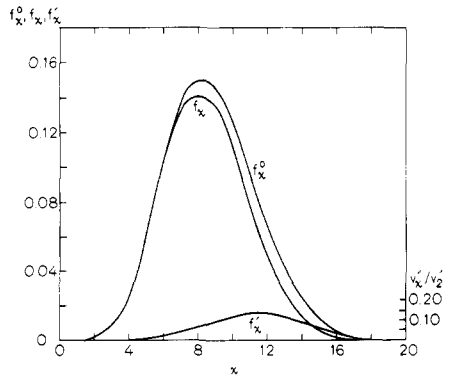

Figure 2. Partitioning of species for $\nu = 7$ at a dilution such that the isotropic phase comprises a fraction $\Phi = 0.90$ of the total volume. See legend to Figure 1.

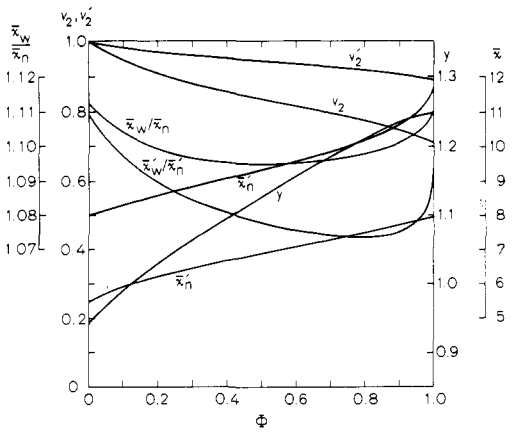

Figure 3. Concentrations v_2 and v_2' and other parameters characterizing the phase equilibria for the Poisson distribution with $\nu = 7$ ($\bar{x}_n^0 = 8$) plotted as functions of the fractional volume Φ of the isotropic phase.

apparent in the displacements of the curves along the abscissa.

Results calculated for partitioning of the parent distribution with $\nu = 7$ at various values of Φ are summarized in Table I and in Figure 3. The value of ν is very close to $\nu = 6.9405$ (see above) for incipience of an isotropic phase in the undiluted system. Hence, v_2 and v_2' are very near unity for $\Phi = 0$. The various quantities plotted in Figure 3 proceed smoothly to finite limits. Peculiarities such as were found for the most probable distribution (see 3) do not occur when $1 - \Phi$ approaches zero. Trends with Φ are otherwise similar to those for the corresponding quantities calculated for the most probable distribution (compare Figure 4 in part 3), except that the changes with Φ are smaller. The disorder parameter y increases monotonically with Φ. It exceeds unity for all $\Phi > 0.125$; for $\Phi < 0.125$ it falls only slightly below unity.

The ratios $\bar{x}_w/\bar{x}_n$ and $\bar{x}_w'/\bar{x}_n'$ in Table I and Figure 3 are generally somewhat smaller than $\bar{x}_w^0/\bar{x}_n^0 = 1.109375$ for the parent Poisson distribution with $\nu = 7$, as given by eq 3. The ratio $\bar{x}_w'/\bar{x}_n'$ for the anisotropic phase is consistently smaller than $\bar{x}_w^0/\bar{x}_n^0$ for all Φ. The ratio $\bar{x}_w/\bar{x}_n$ for the

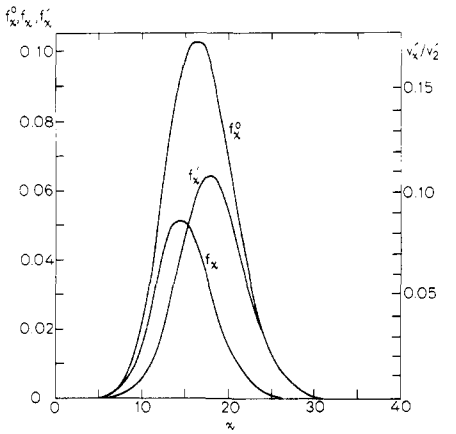

Figure 4. Distributions of species in the coexisting phases, and for the solute as a whole, given that $\bar{x}_n^0 = \nu + 1 = 16$ and $\Phi = 0.50$. See legend to Figure 1.

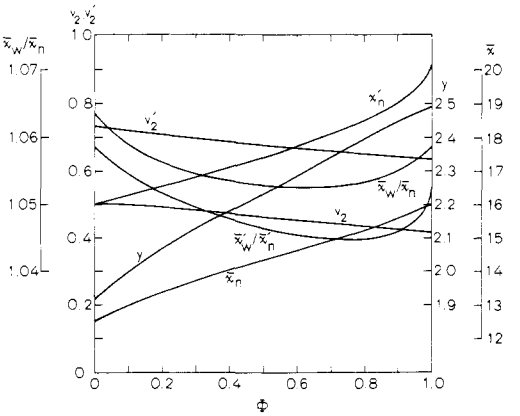

Figure 5. Characteristics of the phases in equilibrium for $\bar{x}_n^0 = \nu + 1 = 6$ as functions of Φ.

isotropic phase exceeds $\bar{x}_w^0/\bar{x}_n^0$ only for $\Phi <$ ca. 0.03. Thus, the distributions in the respective phases are somewhat less polydisperse than Poisson distributions having the same average x, with the exception of the distribution in the isotropic phase within the small range noted. Differences in this respect are much smaller than those found[1] for the most probable distribution. This is consistent with the narrower breadth of the Poisson distribution.

Distributions in the coexisting phases for $\bar{x}_n^0 = \nu + 1 = 16$ and $\Phi = 0.50$ are shown in Figure 4. The main features noted in Figure 1 are repeated. Quantities characterizing the two phases for $\bar{x}_n^0 = 16$ are plotted against Φ in Figure 5. Corresponding quantities calculated for $\bar{x}_n^0 = \nu + 1 = 32$ are shown in Figure 6. Comparisons of Figures 3, 5, and 6 reveal the following trends:

(i) Decreases in the volume fractions v_2 and v_2' with Φ diminish with increase in $\bar{x}_n^0$. The slopes remain negative, however, for all finite values of $\bar{x}_n^0$.

(ii) The values of y and their changes with Φ are roughly proportional to the mean axis ratio $\bar{x}_n^0$.

(iii) The increases in $\bar{x}_n$ and $\bar{x}_n'$ as Φ advances from 0 to 1 increase with $\bar{x}_n^0$, but appear to approach limits; thus the relative changes in $\bar{x}_n$ and $\bar{x}_n'$ with Φ diminish with $\bar{x}_n^0$.

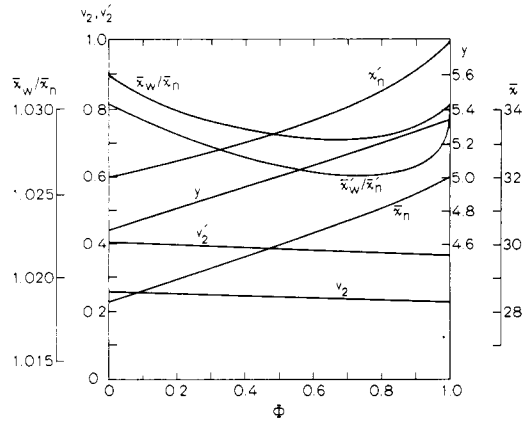

Figure 6. Characteristics of the phases in equilibrium for $\bar{x}_n^0 = \nu + 1 = 32$ as functions of Φ.

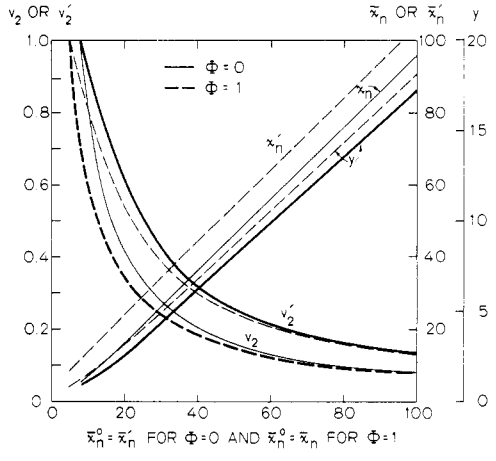

Figure 7. Characteristics of the phases in equilibrium at the limits $\Phi = 0$ (solid curves) and $\Phi = 1$ (dashed curves) plotted against the average axis ratio in the parent phase; i.e., the abscissa expresses $\bar{x}_n' = \bar{x}_n^0$ for $\Phi = 0$ (solid lines) and $\bar{x}_n = \bar{x}_n^0$ for $\Phi = 1$ (dashed lines). Heavy-lined curves represent the parent phases, at $\Phi = 0$ and $\Phi = 1$, respectively, and light-lined curves the respective incipient phases.

(iv) The ratios $\bar{x}_w'/\bar{x}_n'$ for $\bar{x}_n^0 = 16$ ($\nu = 15$) and for $\bar{x}_n^0 = 32$ ($\nu = 31$) are uniformly less than $\bar{x}_w^0/\bar{x}_n^0$ throughout the range $0 < \Phi < 1$. The ranges of Φ commencing at $\Phi = 0$ over which $\bar{x}_w/\bar{x}_n$ exceeds $\bar{x}_w^0/\bar{x}_n^0$ (equal to the intercept of $\bar{x}_w'/\bar{x}_n'$ at $\Phi = 0$, or of $\bar{x}_w/\bar{x}_n$ at $\Phi = 1$) increases with ν, as is apparent from comparison of Figures 3, 5, and 6. At intermediate values of Φ the departures of these ratios from $\bar{x}_w^0/\bar{x}_n^0$, expressed as fractions of $(\bar{x}_w^0/\bar{x}_n^0) - 1$, diminish with increase in $\bar{x}_n^0$ and, hence, with the concomitant decrease in the polydispersity of the parent distribution as measured by $(\bar{x}_w^0/\bar{x}_n^0) - 1$; see eq 3. Thus, selective partitioning of species between the two phases becomes less effective in refining the distribution as the parent distribution is made narrower by increasing its mean axis ratio.

In Figure 7 we show v_2 and v_2' for the coexisting phases at $\Phi = 0$ (solid lines) and at $\Phi = 1$ (dashed lines) plotted against $\bar{x}_n^0$ for the parent phases at these two limits. The lower dashed line is the locus of threshold volume fractions v_2 above which an anisotropic phase separates. The upper solid line is the locus of v_2' below which a conjugate isotropic phase makes its appearance. These two threshold curves are heavy lined. Curves for the volume fractions in the conjugate incipient phases are light lined. The vertical spread between the threshold curves measures the biphasic gap, i.e., the range over which the system is heterogeneous. (For $5.16 < \bar{x}_n^0 < 7.94$ the upper limit is of course $v_2' = 1$.) For $\bar{x}_n^0 = 8$, 16, and 32, the biphasic gap is given also by the difference between v_2' at $\Phi = 0$ and v_2 at $\Phi = 1.0$ in Figures 3, 5, and 6, respectively. It is much smaller than for the most probable distribution, as may readily be seen by inspection of Figures 4 and 8 in part 3.

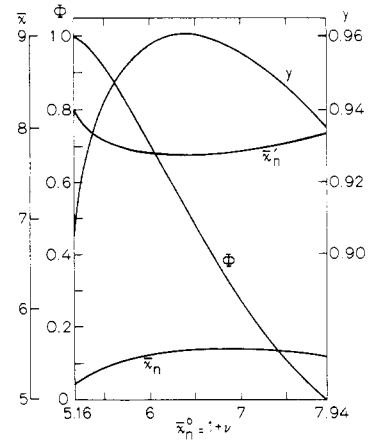

Figure 8. Phase equilibria in undiluted Poisson distributions over the range of $\bar{x}_n^0$ within which biphasic equilibrium obtains.

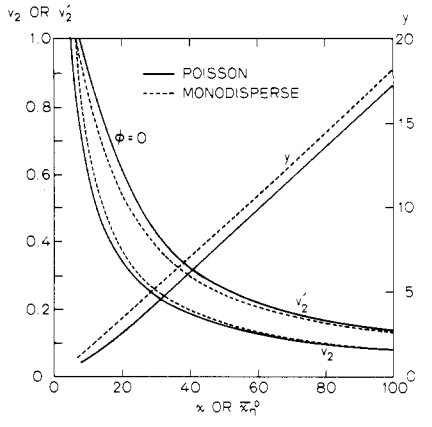

Figure 9. Comparison of thresholds for Poisson distributions (solid curves) with those for monodisperse systems (dashed curves). The solid curves for v_2 and v_2' (Poisson distribution) are identical with the heavy-lined curves, dashed and solid, respectively, in Figure 7. Disorder parameters y for the Poisson distributions and for monodisperse systems also are shown.

Also included in Figure 7 are curves for $\bar{x}_n$ in the incipient isotropic phase at $\Phi = 0$, for $\bar{x}_n'$ in the incipient anisotropic phase at $\Phi = 1$, for y in the parent anisotropic phase at $\Phi = 0$ (heavy lined), and for y in the incipient anisotropic phase at $\Phi = 1$ (light lined).

The curves in Figure 7 for incipience of anisotropic ($\Phi = 1$) and of isotropic ($\Phi = 0$) phases terminate on the ordinate for a volume fraction of unity at $\bar{x}_n^0 = 5.164$ and 7.941, respectively, as deduced in the preceding section. Poisson distributions having mean axis ratios within this range are predicted to be biphasic without dilution. The corresponding range for the most probable distribution,[1] $\bar{x}_n^0 = 2.31$ to 17.76 (calculated for $y = y_{eq}$), is very much broader.

Figure 8 covers the biphasic range for undiluted Poisson distributions. Dependences of $\bar{x}_n$, $\bar{x}_n'$, and y on $\bar{x}_n^0$ are similar to those shown in Figure 10, part 3, for most probable distributions over their biphasic range. Changes in these quantities are smaller for the Poisson distribution, however, in keeping with the more limited range of $\bar{x}_n^0$ over which this distribution is calculated to be biphasic without dilution.

Poisson distributions are compared with monodisperse systems[4] in Figure 9. The two solid curves for v_2 and v_2',

respectively, reproduce the heavy lined threshold curves in Figure 7. The dashed lines show v_2 and v_2' for conjugate phases in the monodisperse system as functions of the axis ratio x. Values of the disorder parameter for the respective systems, also shown in Figure 9, are similar. The dashed lines for v_2' and v_2 for monodisperse systems fall between those for the Poisson distribution for finite values of the (mean) axis ratio. As expected, the biphasic gap measured by the vertical distance between the pair of curves is greater for the Poisson distribution than for the monodisperse system with $x = \bar{x}_n^0$. With increase in $\bar{x}_n^0$ this difference diminishes. The curves for v_2 converge as $\bar{x}_n^0 \rightarrow \infty$; the curves for v_2' also converge, although somewhat more slowly. Hence, the ratio v_2'/v_2, representing the ratio of the phase gap concentrations, proceeds to the common limit, 1.5923.[1,4] Thus, the phase behavior for the Poisson distribution converges to that for the monodisperse solute as x increases. This is, of course, consistent with the diminishing relative breadth of the Poisson distribution with increase in its mean.

Acknowledgment. This work was supported by the Directorate of Chemical Sciences, Air Force Office of Scientific Research, Grant No. 77-3293.

References and Notes

(1) P. J. Flory and R. S. Frost, *Macromolecules*, companion paper in this issue, part 3.
(2) P. J. Flory, "Principles of Polymer Chemistry", Cornell University Press, Ithaca, N.Y., 1953, pp 336–9.
(3) P. J. Flory and A. Abe, *Macromolecules*, companion paper in this issue, part 1.
(4) P. J. Flory, *Proc. R. Soc. London, Ser A*, **234**, 73 (1956).

Statistical Thermodynamics of Mixtures of Rodlike Particles. 5. Mixtures with Random Coils

Paul J. Flory

Department of Chemistry, Stanford University, Stanford, California 94305.
Received June 8, 1978

ABSTRACT: Ternary systems consisting of a solvent (1), a rigid rod solute (2), and a randomly coiled polymer chain (3) are treated according to the model and procedures employed in part 1. Phase equilibria are calculated for systems specified by (x_2,x_3) = (10,10), (20,20), (20,∞), and (100,100), where x_2 and x_3 are the molar volumes of the respective solutes relative to the solvent. Addition of component 3 to the binary system 1,2 increases the volume fraction v_2' of the rodlike solute in the anisotropic phase and broadens the biphasic gap. The preponderance of component 3 is retained by the isotropic phase. Its volume fraction v_3' in the anisotropic phase is $<10^{-4}$ for all compositions and becomes vanishingly small if v_2' is much increased by raising v_3 in the isotropic phase. The isotropic phase exhibits a somewhat greater tolerance for the rodlike component (2). For large values of x_2 and v_3, however, v_2 becomes negligible. The marked segregation of these components between the two phases underscores the basic differences in their mixing tendencies.

Ternary systems comprising an isodiametrical solvent (1), a rodlike solute (2), and a random-coiled chain (3) are considered in this paper. The diameters of components 2 and 3 are assumed equal to that of the solvent. The axis ratio of 2 is x_2 and the contour length of 3 is x_3; i.e., the molecular volumes of the components are in the ratio $1:x_2:x_3$. The theory elaborated in part 1[1] of this series is readily adapted to systems of this description.

The solutes of the ternary systems treated in this paper represent extremes. The one consists of rigid particles of well-defined geometrical form and the other of molecules possessing a substantial degree of flexibility, which therefore assume highly irregular spatial configurations. The profound differences in their mixing behavior are reflected in their limited compatibility with one another. Partitioning of the solute components between nematic and isotropic phases in equilibrium is reminiscent of the "fractionation" of the pairs of rodlike solutes differing in axis ratio considered in paper 2.[2] It is even more marked, however, than for the systems encountered in 2.

Again, the treatment is restricted to "athermal" mixtures or, stated more precisely, to systems in which the exchange free energy is null.

Theory

Combinatorial analysis of the ternary system identified above by use of the lattice model along the lines followed in 1[1,3] yields for the mixing partition function

$$Z_M = \left\{\frac{[n_0 - n_2(x_2 - y)]!y^{2n_2}}{(n_0 - x_2n_2)!n_2!n_0^{n_2(y-1)}}\right\} \times \left\{\frac{(n_0 - x_2n_2)!z_3^{n_3}}{(n_0 - x_2n_2 - x_3n_3)!n_3!n_0^{n_3(x_3-1)}}\right\} \quad (1)$$

$$Z_M = \frac{[n_0 - n_2(x_2 - y)]!y^{2n_2}z_3^{n_3}}{n_1!n_2!n_3!n_0^{n_2(y-1)+n_3(x_3-1)}} \quad (2)$$

where

$$n_0 = n_1 + n_2x_2 + n_3x_3 \quad (3)$$

and z_3 is the internal configuration partition function for the ramdon coil. The first factor in braces in eq 1 expresses the expected number of configurations for the rodlike species in the empty lattice. It corresponds to eq 1-8 as applied to a monodisperse solute. The second term in eq 1 takes account of the configurations accessible to the n_3 random coils subsequently added to the lattice. Introduction of Stirling's approximations for the factorials leads to

$$-\ln Z_M = n_1 \ln v_1 + n_2 \ln v_2 + n_3 \ln v_3 - n_0[1 - v_2(1 - y/x_2)] \ln [1 - v_2(1 - y/x_2)] + n_2(y - 1) - n_2 \ln (x_2y^2) + n_3(x_3 - 1) - n_3 \ln (x_3z_3)] \quad (4)$$

where v_1, v_2, and v_3 are the volume fractions of the respective components.

0024-9297/78/2211-1138$01.00/0